HHS Public Access

Author manuscript

*Neurotoxicology*. Author manuscript; available in PMC 2019 May 01.

Published in final edited form as:

*Neurotoxicology*. 2018 May ; 66: 170–178. doi:10.1016/j.neuro.2017.11.009.

# A Magnetic Resonance Imaging Study of Early Brain Injury in a Rat Model of Acute DFP Intoxication

**Brad A. Hobson**[a], **Douglas R. Rowland**[b], **Suangsuda Supasai**[a], **Danielle J Harvey**[c], **Pamela J Lein**[a], and **Joel R. Garbow**[d]

[a]Department of Molecular Biosciences, University of California, Davis, School of Veterinary Medicine, Davis, CA 95616

[b]Center for Molecular and Genomic Imaging, University of California, Davis, College of Engineering, Davis, CA 95616

[c]Department of Public Health Sciences University of California, Davis, School of Medicine, Davis, California 95616

[d]Biomedical Magnetic Resonance Laboratory, Mallinckrodt Institute of Radiology, School of Medicine, Washington University in St. Louis, St. Louis, Missouri 63110

## Abstract

Current treatments for seizures induced by organophosphates do not protect sufficiently against progressive neurodegeneration or delayed cognitive impairment. Developing more effective therapeutic approaches has been challenging because the pathogenesis of these delayed consequences is poorly defined. Using magnetic resonance imaging (MRI), we previously reported brain lesions that persist for months in a rat model of acute intoxication with the OP, diisopropylfluorophosphate (DFP). However, the early spatiotemporal progression of these lesions remains unknown. To address this data gap, we used *in vivo* MRI to longitudinally monitor brain lesions during the first 3 d following acute DFP intoxication. Adult male Sprague Dawley rats acutely intoxicated with DFP (4 mg/kg, sc) were MR imaged at 6, 12, 18, 24, 48, 72 h post-DFP, and their brains then taken for correlative histology to assess neurodegeneration using FluoroJade C (FJC) staining. Acute DFP intoxication elicited moderate-to-severe seizure activity. T2-weighted (T2w) anatomic imaging revealed prominent lesions within the thalamus, piriform cortex, cerebral cortex, hippocampus, corpus striatum, and substantia nigra that corresponded to neurodegeneration, evident as bands of FJC positive cells. Semi-quantitative assessment of lesion severity demonstrated significant regional variation in the onset and progression of injury, and suggested that lesion severity may be modulated by isoflurane anesthesia. These results imply that the timing of therapeutic intervention for attenuating brain injury following OP intoxication may

**Co-Corresponding authors:** Pamela J. Lein, Molecular Biosciences, University of California, Davis, 1089 Veterinary Medicine Drive, Davis, CA 95616, pjlein@ucdavis.edu, Office phone: 539-752-1970, Joel R. Garbow, Biomedical MR Laboratory, Washington University School of Medicine, Campus Box 8227, 4525 Scott Avenue, St. Louis, MO 63110, garbow@wustl.edu, Office phone: (314) 362-9949.

be regionally dependent, and that longitudinal assessment of OP-induced damage by MRI may be a powerful tool for assessing therapeutic response.

**Keywords**

*In vivo* imaging; neuropathology; organophosphate; seizure; T2-weighted MRI

## 1.0 Introduction

Organophosphate anticholinesterases (OPs) are potent neurotoxicants that are widely used as pesticides, and have been developed as nerve agents (e.g., sarin and soman) (Gupta, 2006). OP intoxication is estimated to cause over 170,000 deaths and 1 million life-threatening intoxications each year (Gunnell et al., 2007, Mew et al., 2017). These statistics, coupled with the documented use of OP nerve agents by governments (Dolgin, 2013) and terrorist organizations (Morita et al., 1995), identify OPs as a serious public health threat (Gunnell and Eddleston, 2003, Jett, 2007, Pereira et al., 2014). Acute intoxication with high doses of OPs quickly leads to irreversible inhibition of acetylcholinesterase within the brain and periphery, which causes cholinergic crisis and can trigger seizures that rapidly progress to *status epilepticus* (SE) (Chen, 2012, Collombet, 2011, Lowenstein et al., 1999). Preclinical studies of OP-induced SE have demonstrated the development of profound neuropathology, including extensive neuronal necrosis and neuroinflammation, in the days following OP intoxication that can persist for weeks to months post-exposure (Aroniadou-Anderjaska et al., 2016, Chen, 2012, Collombet, 2011, Flannery et al., 2016, Li et al., 2011, Liu et al., 2012, Siso et al., 2017). Clinical case studies and preclinical models also indicate lasting neurologic consequences, including brain atrophy, loss of cognitive function, memory deficits, and epilepsy that develops after a latent period following OP-induced SE (Aroniadou-Anderjaska et al., 2016, Chen, 2012, Flannery et al., 2016, Hobson et al., 2017, Miyaki et al., 2005).

Current antidotes are of limited use in treating acute OP intoxication because unless administered within minutes after exposure, they neither effectively terminate seizures nor prevent the ensuing neuropathology and chronic neurological consequences (Collombet, 2011, McDonough et al., 2010). There is, therefore, an urgent need for more effective treatments. Electroencephalographic and neuropathological data suggest that the hours following acute intoxication are likely critical therapeutic windows for mitigating subsequent morbidity (Kaur et al., 2014). However, the optimal timing for the delivery of potential therapeutics remains poorly defined, due in part to: (i) a paucity of systematic, longitudinal data on the progression of OP intoxication-induced brain damage; and (ii) a limited understanding of the degree to which structurally diverse OP nerve agents and pesticides share common spatiotemporal profiles of injury. Addressing these challenges using classic, terminal histologic methods can be time-consuming and cost-prohibitive because of the number of animals required and the extensive tissue processing needed for comprehensive spatiotemporal assessment of the brain. One strategy for overcoming these challenges is to use non-invasive imaging modalities, such as magnetic resonance imaging (MRI).

MRI has been a valuable tool for studying the consequences of seizures (Mendes and Sampaio, 2016, Milligan et al., 2009). Using MRI, the rodent brain can be noninvasively and repeatedly interrogated, enabling detailed spatiotemporal mapping of brain injury within a single animal. In addition to reducing animal numbers, the collection of longitudinal data increases statistical power and allows animals with varying response patterns to be readily identified. While MRI has been used extensively to study preclinical seizure models, there are a limited number of publications describing the use of MRI to assess seizure-induced brain injury in preclinical models of acute OP intoxication (Bhagat et al., 2001, Bhagat et al., 2005, Carpentier et al., 2008, Gullapalli et al., 2010, Hobson et al., 2017, Rosman et al., 2012, Shrot et al., 2012, Shrot et al., 2015, Testylier et al., 2007). We recently reported a correlative histologic and MRI-based characterization of a rat model of acute intoxication with the OP pesticide, diisopropylfluorophosphate (DFP) (Hobson et al., 2017, Siso et al., 2017). Similar to OP nerve agents, DFP rapidly produces SE, as determined by electroencephalography (Pouliot et al., 2016), and generates progressive neuronal necrosis (Siso et al., 2017), neuroinflammation (Flannery et al., 2016), and cognitive impairment (Brewer et al., 2013, Flannery et al., 2016). In our previous MRI studies, we characterized the progression of brain lesions beginning at 3 d out to 1 month post-DFP intoxication. However, there are no MRI data published regarding lesion development during the first 3 d following DFP intoxication. While previous MRI studies in rodent models of acute intoxication with OP nerve agents have detected lesions as early as 3 h post-intoxication (Carpentier et al., 2008, Shrot et al., 2012), considerable variation in injury has been reported at these early time points. It is unclear, however, whether these disparate findings reflect differences in the intoxicating OP (soman *vs.* sarin) *vs.* differences in the time at which images were collected post-exposure. Distinguishing between these possibilities is difficult given that few studies have examined more than one time point during the first 24 h following OP intoxication (Bhagat et al., 2005).

The objective of the current study was to address the gap in knowledge regarding the progression of brain injury during early time points post-exposure after OP-induced SE by generating a spatiotemporal profile of brain lesions detected during the first 72 h following DFP exposure by anatomic, T2-weighted (T2w) MR imaging.

## 2.0 Methods

### 2.1 Animals and DFP exposures

All animals were housed in facilities fully accredited by AAALAC Internatonal, and all studies were performed with regard to the alleviation of pain and suffering under protocols approved by the University of California-Davis Institutional Animal Care and Use Committee. Adult male Sprague Dawley rats (250–280g; Charles River Laboratories, Hollister, CA) were housed individually in standard plastic shoebox cages under controlled environmental conditions (22 ± 2 °C, 40–50% humidity) with a normal 12 h light/dark cycle. Food and water were provided *ad libitum*.

DFP (> 90% purity as determined by $^{1}$H-NMR spectroscopy) was purchased from Sigma Chemical Company (Saint Louis, MO) and upon opening a sealed vial, was aliquoted and stored at −80°C. Under these conditions, it has been shown that DFP is stable for at least 400

days (Heiss et al., 2016). DFP was diluted with sterile, ice-cold phosphate buffered saline (PBS) within 5 min of administration to unanesthetized rats at 4 mg/kg in a total volume of 300 μl via sc injection. In addition, animals received 0.1 mg/kg pyridostigmine bromide (TCI America, Portland, OR), im, 30 min prior to DFP administration and immediately following DFP exposure, rats were injected with atropine sulfate (Sigma Chemical Company) at 2.0 mg/kg, im, and pralidoxime (2-PAM, Sigma Chemical Company) at 25 mg/kg in saline, im. These treatments significantly reduce mortality by blocking the peripheral parasympathomimetic clinical signs associated with acute OP intoxication (Kim *et al.*, 1999). This dosing paradigm has been shown to reliably produce sustained seizures in > 90% of injected animals with > 75% survival of seizing animals at 24 h post-DFP injection (Pessah et al., 2016). At 4 h post-exposure, animals were injected sc with 10 ml of 5% dextrose in saline to replace lost fluids and to prevent hypoglycemia, and returned to their home cages where they were provided with rat chow softened in water for the duration of the study.

### 2.2 Scoring seizure behavior

Seizure severity was quantified as previously described (Hobson et al., 2017, Siso et al., 2017) using a five-point cholinergic toxicity scale based on the following behavioral criteria: 0, no clinical signs; 1, salivation, urination, lacrimation and/or defecation (SLUD); 2, muscle fasciculations and tremors; 3, forelimbs clonus; 4, rearing and hindlimb clonus; 5, rearing with falling and loss of righting reflex. Repeated scores of three and above were shown previously in a preclinical model of acute DFP intoxication to correspond to *SE*, defined as sustained seizure activity detected by electroencephalography that persists for more than 5 min (Deshpande et al., 2010, Pouliot et al., 2016). Seizure behavior was scored at 5 min intervals from 0–120 min post-DFP intoxication, and at 20 min intervals from 120–240 min post-DFP (Figure S1 in supplementary material). Animals achieving scores of ≥ 3 at multiple consecutive time points were included in the MRI study. Of a total of twenty injected animals, the twelve animals with the highest average cholinergic toxicity scores over 4 h post-DFP injection were selected for the MRI study (individual animal seizure scores for all 20 animals are provided in Table S1 in supplementary material).

### 2.3 *In vivo* magnetic resonance imaging and analysis

MRI scans were performed at the Center for Molecular and Genomic Imaging, using a Bruker Biospec 70/30 (7T) preclinical MR scanner (Bruker BioSpin MRI, Ettlingen Germany) equipped with a 116-mm internal diameter B-GA12S gradient (450 mT/m, 4,500 T/m/s), a 72-mm internal diameter linear transmit coil, and a four-channel, rat-brain phased array in crossed coil configuration for signal reception. Images were acquired and reconstructed using Paravision 5.1 (Bruker BioSpin, MRI). Multislice, T2w, Rapid Acquisition with Repeated Echoes (RARE) transaxial images were collected over 10 min, using the following parameters: repetition time (TR) = 6100 ms; effective echo time (TE) = 60 ms; RARE factor = 8; averages = 4; field of view (FOV) = 35 × 25 $mm^2$, in-plane data matrix = 280 × 200, resulting in an in-plane pixel resolution of 0.125 × 0.125 $mm^2$ for 44 slices with a 0.5-mm thickness, spanning approximately 8.0 to −14.0 mm bregma according to Paxinos and Watson's *The Rat Brain in Stereotaxic Coordinates* (Paxinos, 2007). Animals were randomly divided into two groups prior to imaging: Group 1 animals, which were

imaged at 6, 18, 48, and 72 h post-DFP injection; and Group 2 animals, which were imaged at 12, 24, and 72 h post-DFP injection. To account for the 90 min required to complete imaging of the six animals within each group, scanning began 45 min prior to, and ended 45 min after nominal time points (e.g., the imaging time for Group 1 at the nominal time point of 6 h was 6 ± 0.75 h). A vehicle control animal similarly treated with pyridostigmine bromide, atropine and 2-PAM but injected with 300 μl of PBS in place of DFP, was imaged at 72 h to provide an anatomic reference and baseline for scoring lesion severity, as discussed below. Immediately prior to imaging, animals were placed in a Plexiglas induction chamber and anesthetized with isoflurane/$O_2$ (Piramal Healthcare, Bethlehem PA), 2.0–3.0% vol/vol for 3–5 min. After induction, animals were secured in a custom stereotactic head restraint, anesthesia was reduced to 1.0–2.0% vol/vol, and animals were then placed in the MR scanner (2–5 min). Once in the scanner, a body temperature of 37°C and respiration rate of 50–70 breaths/min were maintained using warm air and adjustment of isoflurane levels. Temperature and respiration rate were monitored using SAII 1025T small-animal monitoring equipment (Small Animal Instruments, Inc., Stony Brook, NY). Animals were in the scanner for 10–15 min for image localization and RARE scans.

Delineation of brain regions was guided by Paxinos and Watson's *The Rat Brain in Stereotaxic Coordinates* (Paxinos, 2007), and eight regions were agreed upon prior to scoring of lesion severity. The axial extent of assessed brain regions, defined as the "anterior start distance from bregma"/"extent in mm", were: cerebral cortex, 2.0/7.0; hippocampus, −2.5/3.5; lateral ventricles, 2.0/7/0; piriform cortex, 2.0/5.0; caudate putamen, 2.0/3.5; globus pallidus, 0.5/1.5; substantia nigra, −5.0/1.0; and thalamus (medial and dorsolateral), −1.5/2.5.

Changes in T2w images induced by acute DFP-intoxication, hereafter referred to as lesions, were identified in T2w images based on their hyperintensity relative to neighboring tissue and the corresponding brain region on T2w images of historical vehicle controls 72 h post-exposure (Hobson et al., 2017). Regional lesion severity was scored by two independent observers blinded to seizure severity, using a multiparametric scale ranging from 0 to 3, according to the following criteria: 0, no hyperintensity; 1, hyperintensity the extent of which was < 50% of assessed region of interest (ROI); 2, either stark hyperintensity with distinct discrete borders, *or* hyperintensity the extent of which was > 50% of the assessed ROI; 3, both stark hyperintensity with distinct discrete borders *and* hyperintensity that covered > 50% of the ROI. Lateral ventriculomegaly was scored based on the following visual criteria: 0, no ventricular enlargement, 1, bilateral ventricular enlargement < 2 times vehicle control reference; 2, unilateral enlargement ≥ 2 times vehicle control reference; 3, bilateral enlargement ≥ 2 times vehicle control reference. Representative T2w images illustrating lesions scored according to these criteria are presented in the supplementary material (Figure S2). Half-unit increments were used when definitive integer scores were ambiguous. Lesions were bilateral, but occasionally varied in severity between hemispheres. This hemispheric variation was taken into account during the scoring of lesion severity in which a single score was determined for the combined hemispheres of a given brain region. Individual scores between raters differed by ≤ 1.0, with an average difference between scores of 0.23 ± 0.27 and overall inter-rater reliability of 0.745, as determined using Fleiss's Kappa with linear weighting. Final regional lesion severity scores used for statistical

analyses were the averages of the individual observer scores per region/by animal/by time point. The lesion scoring data for the twelve animals included in the MRI study are provided in the supplementary material (Table S2).

### 2.4 Histology

Brains were harvested at 3 d post-exposure from animals deeply anesthetized with 4% isoflurane in oxygen, and subsequently perfused transcardially with 100 ml cold PBS at a rate of 15 ml/min using a Masterflex peristaltic pump (Cole Parmer, Vernon Hills, IL) followed by 100 ml cold 4% paraformaldehyde (aq). Brains were serially trimmed into 2.0 mm blocks, post-fixed in 4% paraformaldehyde (aq) at 4°C for 24 h, and then transferred to 30% sucrose in PBS. Brains were stored in 30% sucrose at 4°C at least until they had sunk to the bottom of the vial. Brain blocks were embedded in O.C.T. compound (Sakura Finetek, Torrance, CA), flash frozen and then sectioned into 10 μm thick axial slices that were stored at −80°C until further processed. To detect neuronal degeneration, sections were labeled with FluoroJade C (FJC) (Millipore, Billerica, MA), as previously described (Li et al., 2011), with minor modifications. Briefly, after air drying, sections were washed with distilled water and then directly incubated in 0.03% potassium permanganate (KMnO4) (aq) for 10 min on a shaker table, followed by distilled water for 2 min. Sections were then incubated in a freshly prepared solution of 0.00015% FJC in 0.1% acetic acid (aq) for 10 min, rinsed in distilled water and then dried at 50°C. Dried slides were cleared by immersion in xylene for 2 min before cover slipping in Permount (Fisher Scientific, Hampton, NH).

### 2.5 Statistics

The primary outcome was the average of two independent ratings of lesions in MR images across multiple regions of the brain (cerebral cortex, hippocampus, thalamus, and piriform cortex) over time, for each animal in two different cohorts of DFP- exposed animals. Due to the repeated measures across regions and across time for each animal, mixed-effects regression models were used to assess the overall mean trajectories of lesion severity over time, as well as differences by brain region and cohort. Time, in days post-exposure, was treated as a continuous variable in the model (e.g., a fixed effect) to capture the pattern of lesion severity over time. The coefficient for time may be interpreted as the average change in lesion severity per day. Individual trajectories of animals (supplementary material, Figure S3), as well as model diagnostics including residual plots, indicated a quadratic association with time. To account for this non-linearity, a term for time squared was also included as a fixed effect in the models, which taken together with the term for time describes the quadratic pattern of lesion severity. A negative coefficient of time squared indicates a “hill-like” pattern, while a positive coefficient suggest a “valley-like” pattern. Fixed effects for brain region and cohort were included to assess the associations between brain region or cohort and level of lesion severity. Further, interactions between region or cohort and the time variables were assessed to evaluate the differences in the temporal trends (quadratic pattern) by brain region or cohort. The animal-specific random effect accounts for unexplained biological heterogeneity, such that some animals may inherently be more susceptible to lesions even after accounting for the fixed effects, such as brain region and cohort, while others may be resistant to lesions.

Model building began with the full model considering all main effects (such as brain region, cohort, time and time-squared) as well as the interactions between brain region and cohort and the time variables. Interactions were dropped individually and these reduced models were compared to the full model using the Akaike information criterion (smaller is better) until the Akaike information criteria was no longer reduced. This final model was then used to characterize the spatiotemporal patterns of lesion severity by group. Contrasts specifically comparing the two cohorts were created and used to statistically test for differences between the groups. 95% confidence intervals for the slope (coefficient for time) and for the coefficient of time-squared for each brain region were also obtained from the model. All analyses were conducted using SAS version 9.4, and graphics were created in R, version 3.1.0.

## 3.0 Results

### 3.1 DFP intoxication produces robust seizures consistent with *status epilepticus*

Consistent with our previous studies (Flannery et al., 2016, Hobson et al., 2017, Siso et al., 2017), acute DFP-intoxication resulted in behavioral signs of seizure activity consistent with SE in the twelve animals included in the MRI study. There was no significant difference in average cholinergic toxicity scores between animals in Group 1 (2.99 ± 0.13) *vs.* Group 2 (2.84 ± 0.31) (the average cholinergic toxicity score for each individual animal is provided in the supplementary material, Table S1). Behavioral signs of seizure attenuated to levels below those suggestive of SE (cholinergic toxicity score ≤ 2) by the start of imaging at 6 h post-exposure, and were back to vehicle control levels by the initiation of imaging at 12 h post-exposure. The survival rate was ~92%, with one animal in Group 1 dying between 24 and 48 h post-DFP injection.

### 3.2 DFP intoxication results in progressive brain lesions detected by T2w MRI

MRI imaging revealed bilateral lesions following acute DFP intoxication. Lesions were characterized by T2w hyperintensity in limbic brain regions (i.e., hippocampus, piriform cortex, thalamus, amygdala, basal ganglia) and cerebral cortex (spanning the complete somatosensory cortex, and portions of the motor, auditory, and parietal and visual cortices) that varied both spatially and temporally (Figure 1). At first appearance, lesions were localized along tissue subregions, i.e., banded layers of the piriform cortex or the dorsal aspect of the CA1 within the hippocampus (Figure 1). Overall, lesions were defined by discrete, hyperintense foci with defined borders that initially expanded in area (became more extensive) over time, and then later decreased in size (extent) and intensity, and exhibited less defined lesion borders.

At the earliest imaging time point (6 h post-DFP injection in Group 1 animals), lesions were consistently observed within the thalamus and cerebral cortex, and more variably within the piriform, globus pallidus and substantia nigra (Figures 1, 2, and Table 1). When present, lesions were most extensive and intense in the thalamus, followed by the substantia nigra, and were comparatively less extensive and intense in the cerebral cortex, piriform cortex, septal area, and amygdala. Lesions were notably absent in the hippocampus, caudate putamen, and elsewhere in the brain. Similarly, lesions at 12 h post-intoxication, the first

imaging time point of Group 2 animals, were significantly more severe ($p<0.001$) in the thalamus than in the piriform and cerebral cortices. Lesions in these three brain regions were significantly more severe ($p<0.001$) than the variable lesions in the hippocampus. At the 12 h time point, ventriculomegaly was also observed, which persisted in a subset of animals for the remainder of the study (Table 1).

At subsequent time, 18 h for Group 1 and 24 h for Group 2, lesions within the piriform cortex, hippocampus, cerebral cortex, and thalamus either did not change or increased in extent and/or severity, with the exception of decreased lesion severity in the thalamus of Group 2 animals ($p<0.001$). Strikingly, at 18 h post-DFP injection, Group 1 animals developed significant lesions within the caudate putamen that were not observed in Group 2 animals at 24 h. By 48 h post intoxication, lesions in Group 1 animals were attenuated within the thalamus, caudate putamen, and cerebral cortex, but increased in severity in the piriform cortex and hippocampus. At 72 h, in both imaging groups, lesions were common in the hippocampus, piriform cortex, and thalamus, variably apparent in the cerebral cortex, and only occasionally observed within the globus pallidus, substantia nigra and caudate putamen (Table 1). Overall, lesion severity decreased across brain regions by 72 h post-intoxication, with the marked exception of the hippocampus, which showed increased lesion severity at 72 h post-DFP injection (Table 1).

After imaging was completed at 72 h, animals were euthanized to collect brains for histological confirmation of neuropathology using FJC staining. Consistent spatial registry was observed between the location of hyperintense lesions in T2w images and regions of neurodegeneration as determined by FJC staining (Figure 3): the piriform cortex (11/11), cerebral cortex (somatosensory) (11/11), hippocampus (CA1, CA3, dentate gyrus) (9/9), and thalamus (9/9) (Figure 3). Conversely, no FJC staining was observed in regions in which no lesions were detected by MRI.

### 3.3 Quantitative analysis reveals that T2w MRI lesion severity varies according to brain region, time post-exposure and group

To further characterize our observational findings, lesion scoring in the hippocampus, thalamus, piriform and cerebral cortices was subjected to mixed-model regression analysis. Overall, average lesion severity varied significantly between imaging groups, brain regions and time post-exposure (Figure 4). With respect to inter-group differences, Group 1 had lower average lesion severity scores over the study period than Group 2 in the thalamus ((95% CI: −1.6, −0.5) and the piriform cortex (95% CI: −1.3, −0.1); however, in all other brain regions, scores were similar between imaging groups over time. In terms of spatiotemporal variation, patterns were similar for the two imaging groups. Lesions in the piriform cortex showed an initial increase in severity (slope 95% CI: 1.4, 2.6); however, lesion severity eventually peaked and then started to attenuate (time-squared 95% CI: −0.7, −0.4). A similar, but less pronounced, pattern was observed in the cerebral cortex (slope 95% CI: 0.3, 1.3; time-squared 95% CI: −0.5, −0.1). Lesions in the thalamus did not change linearly over time (slope 95% CI: −0.4, 0.6), but, rather, experienced slight curvature (time-squared 95% CI: −0.3, −0.02), suggesting lesion attenuation. In contrast, lesion severity scores in the hippocampus showed no evidence of curvature (time-squared 95% CI: −0.2,

0.2), but tended to increase linearly over time, although the increase narrowly missed statistical significance (slope 95% CI: −0.02, 1.1).

## 4. Discussion

This study represents the most detailed MRI characterization to date of the spatiotemporal progression of brain lesions during the first 72 h following acute OP intoxication. Our data demonstrate that acute DFP intoxication in the rat produces hyperintense lesions in T2w brain images that are detectable as early as 6 h post-exposure, evolve in extent and intensity with time, and overlap spatially to areas of histologically defined neurodegeneration. Lesion onset, severity and changes over time were found to be region-dependent, and possibly influenced by the timing of administration of isoflurane anesthesia.

T2w MRI of DFP-intoxicated animals revealed hyperintense lesions characterized by region-dependent patterns of injury that varied with respect to time-to-onset and pattern of progression. Lesions were apparent as early as 6 h in the thalamus, substantia nigra, and piriform and cerebral cortices while in the caudate putamen and the hippocampus, the onset of injury was delayed until 12 h post-intoxication. Longitudinal analysis of the earliest lesions revealed that their hyperintensity began to attenuate within 3 d post-exposure, while lesions in the hippocampus continued to increase in extent and intensity throughout the 72 h study. These spatiotemporal patterns of DFP-induced T2w lesions are consistent with T2w MRI assessments of soman intoxication in the rat and guinea pig, which reported that the thalamus and piriform cortex were the most severely damaged regions at 3 and 6 h post-intoxication, respectively (Gullapalli et al., 2010, Shrot et al., 2012). Longitudinal analysis of T2w lesion severity in the soman-intoxicated guinea pig (Gullapalli et al., 2010) also demonstrated a delayed onset of more than 24 h in the appearance of hippocampal hyperintensity relative to other damaged regions.

The spatiotemporal distribution of lesions following DFP-induced SE are similar to MRI assessments of other preclinical seizure models, including pilocarpine (Duffy et al., 2014, Roch et al., 2002, Suleymanova et al., 2016), kainic acid (Liachenko et al., 2015, Nakasu et al., 1995), and electrical stimulation (Nairismagi et al., 2004). Studies using these other seizure models have focused on the hippocampus, piriform cortex, and thalamus, and there are few reports of injury in the globus pallidus, caudate putamen, and substantia nigra. However, it is unclear if the latter is unique to our DFP model, or if evidence of damage to the globus pallidus, caudate putamen, and substantia nigra are simply under reported due to the early onset and resolution of T2w lesions in these brain regions. Nonetheless, as suggested earlier (Hobson et al., 2017), the commonalities in spatiotemporal patterns of brain injury across preclinical models of SE that vary with respect to model species and nature of the SE trigger, suggest that brain lesions observed following acute DFP intoxication are primarily due to prolonged seizure activity.

While the etiology of lesions following DFP-induced SE is unclear, contributing mechanisms likely include cerebral edema, hypoxia and excitotoxicity. Previous MRI-based studies of convulsive OP intoxication using DFP or OP nerve agents have demonstrated a high degree of spatial registry between T2w hyperintense lesions and canonical signs of

edema, including transient increases in tissue-water content, restricted water diffusion, tissue vacuolar changes, and subsequent brain atrophy associated with lateral ventricle enlargement (Carpentier et al., 2008, Hobson et al., 2017, Rosman et al., 2012, Testylier et al., 2007). Cerebral edema in preclinical models of SE and traumatic brain injury (Bareyre et al., 1997), is characterized by acute induction of fluid accumulation occurring during the first 24 to 72 h, followed by fluid reabsorption, and then eventual tissue atrophyover days to weeks (Bertoglio et al., 2017, Grohn and Pitkanen, 2007). Similarly, with the exception of the hippocampus, brain lesions following DFP-induced SE initially expand then recede coincident with the development of ventriculomegaly. The T2w lesions observed following acute DFP intoxication are also strikingly similar to those detected by MRI during the first few hours following hypoxia-ischemia in the rat (Farr and Wegener, 2010), and regional differences in tissue hypoxia may represent a source of variation in spatiotemporal patterns of neuropathology following DFP-induced SE. Collectively, observations in the rat model of DFP-induced SE are consistent with the hypothesis that neuropathology following SE in rats proceeds by excitotoxic and ischemic mechanisms (Fabene et al., 2007, Puyal et al., 2013).

Alternatively, the spatiotemporal patterns of lesions observed following OP-induced SE may reflect secondary degeneration, a phenomenon whereby neuronal damage is propagated along specific anatomic routes defined by neural circuits (Myhrer and Aas, 2014). Our data are consistent with previous proposals that early damage in the piriform cortex, which contains a well characterized initiation site for SE, *the area tempestas*, triggers delayed injury in the hippocampus via the perforant pathway (Chen et al., 2014, McDonough and Shih, 1997, Siso et al., 2017). Secondary degeneration may also explain our observation that in DFP-intoxicated animals with lesions in the substantia nigra at 6 h, hyperintensity is subsequently observed within the caudate putamen at 18 h. The substantia nigra, like the *area tempestas*, is a critical initiation point for generalized seizures (Gale, 1988), and, like the piriform cortex, is damaged early following acute DFP intoxication. The substantia nigra *pars compacta* projects extensive dopaminergic connections to the caudate putamen *via* the nigrostriatal pathway (Lanciego et al., 2012). Thus, damage to the substantia nigra may trigger delayed lesions in the caudate putamen. However, neuronal circuitry within the basal ganglia is highly complex, and there are significant connections between the caudate putamen and not only the substantia nigra, but also the thalamus, cerebral cortex, and globus pallidus(Lanciego et al., 2012), all regions damaged early following DFP-induced SE. A more granular profile of the time course of damage in these brain regions over the first 12 h following DFP-induced SE may provide a better understanding of these interactions.

An unexpected finding of this study was the difference in lesion severity observed between the two imaging groups. While the regional patterns of injury progression were the same in both groups, lesion severity in the piriform cortex and thalamus was significantly reduced in Group 1 compared to Group 2. Both imaging groups were subject to the same DFP intoxication paradigm and experienced similar average cholinergic toxicity scores. The primary difference between the groups was the timing and summed duration of isoflurane anesthesia. Group 1 animals received isoflurane anesthesia 6 h earlier than Group 2 animals, and Group 1 animals were imaged over four sessions compared to three sessions for Group 2. The significantly reduced severity of lesions in Group 1 compared to Group 2 suggest a neuroprotective effect from earlier initiation and/or increased total exposure to anesthesia.

Neuroprotective effects of isoflurane have been demonstrated in preclinical models of stroke and traumatic brain injury, as well as preclinical and clinical epilepsy (Bar-Klein et al., 2016, Gaidhani et al., 2017, Hertle et al., 2012, Zeiler et al., 2015). Electroencephalographic characterization of mice acutely intoxicated with soman demonstrated that isoflurane administered for 90 min, beginning 3 h post-soman intoxication, effectively terminates seizures for the duration of general anesthesia, although SE recurred when isoflurane was discontinued (Testylier et al., 2007). Nonetheless, soman-intoxicated animals that received isoflurane exhibited less neuropathology within the piriform cortex compared to unanesthetized animals. Similarly, our data indicate that isoflurane is neuroprotective in a preclinical model of acute DFP intoxication, and suggest that: *(i)* the timing of isoflurane anesthesia influences lesion severity, and/or *(ii)* repeated doses as low as 2% isoflurane for 15 min can significantly affect the manifestation of injury.

In summary, our findings indicate that brain injury is apparent by MRI within hours of DFP-induced SE, although the pattern of injury varies by brain region. The neuroprotective effect of isoflurane administered 6 h after DFP-induced SE suggests the potential for delayed therapeutic interventions to mitigate downstream neurological consequences, but also warns that therapeutic interventions may vary regionally. Thus, while structural changes in the brain may not capture all endpoints of therapeutic relevance in OP-induced SE, our data support longitudinal assessment of OP-induced damage by MRI as a powerful tool for assessing not only OP-induced neuropathology, but also therapeutic response.

## Supplementary Material

Refer to Web version on PubMed Central for supplementary material.

## Acknowledgments

The authors thank Donald Bruun (University of California, Davis) for his assistance with animal care. This work was supported by the National Institutes of Health [CounterACT Program grant number NS079202 and predoctoral fellowship to BH from training grant GM099608]. BH was also supported by a predoctoral fellowship from the David and Dana Loury Foundation and the ARCS Foundation.

## Abbreviations

| | |
|---|---|
| **DFP** | Diisopropylfluorophosphate |
| **FJC** | FluoroJade C |
| **MR** | magnetic resonance |
| **MRI** | Magnetic resonance imaging |
| **OP** | Organophosphate |
| **SE** | *status epilepticus* |
| **T2w** | T2-weighted |

## References


Aroniadou-Anderjaska V, Figueiredo TH, Apland JP, Prager EM, Pidoplichko VI, Miller SL, et al. Long-term neuropathological and behavioral impairments after exposure to nerve agents. Ann N Y Acad Sci. 2016; 1374:17–28. [PubMed: 27002925]

Bar-Klein G, Klee R, Brandt C, Bankstahl M, Bascunana P, Tollner K, et al. Isoflurane prevents acquired epilepsy in rat models of temporal lobe epilepsy. Ann Neurol. 2016; 80:896–908. [PubMed: 27761920]

Bareyre F, Wahl F, McIntosh TK, Stutzmann JM. Time course of cerebral edema after traumatic brain injury in rats: effects of riluzole and mannitol. J Neurotrauma. 1997; 14:839–49. [PubMed: 9421455]

Bertoglio D, Verhaeghe J, Dedeurwaerdere S, Grohn O. Neuroimaging in animal models of epilepsy. Neuroscience. 2017; 358:277–99. [PubMed: 28688882]

Bhagat YA, Obenaus A, Hamilton MG, Kendall EJ. Magnetic resonance imaging predicts neuropathology from soman-mediated seizures in the rodent. Neuroreport. 2001; 12:1481–7. [PubMed: 11388434]

Bhagat YA, Obenaus A, Hamilton MG, Mikler J, Kendall EJ. Neuroprotection from soman-induced seizures in the rodent: evaluation with diffusion- and T2-weighted magnetic resonance imaging. Neurotoxicology. 2005; 26:1001–13. [PubMed: 15982742]

Brewer KL, Troendle MM, Pekman L, Meggs WJ. Naltrexone prevents delayed encephalopathy in rats poisoned with the sarin analogue diisopropylflurophosphate. Am J Emerg Med. 2013; 31:676–9. [PubMed: 23380104]

Carpentier P, Testylier G, Dorandeu F, Segebarth C, Montigon O, Foquin A, et al. Hyperosmolar treatment of soman-induced brain lesions in mice: evaluation of the effects through diffusion-weighted magnetic resonance imaging and through histology. Toxicology. 2008; 253:97–103. [PubMed: 18824071]

Chen Y. Organophosphate-induced brain damage: mechanisms, neuropsychiatric and neurological consequences, and potential therapeutic strategies. Neurotoxicology. 2012; 33:391–400. [PubMed: 22498093]

Chen Y, Garcia GE, Huang W, Constantini S. The involvement of secondary neuronal damage in the development of neuropsychiatric disorders following brain insults. Front Neurol. 2014; 5:22. [PubMed: 24653712]

Collombet JM. Nerve agent intoxication: recent neuropathophysiological findings and subsequent impact on medical management prospects. Toxicol Appl Pharmacol. 2011; 255:229–41. [PubMed: 21791221]

Deshpande LS, Carter DS, Blair RE, DeLorenzo RJ. Development of a prolonged calcium plateau in hippocampal neurons in rats surviving status epilepticus induced by the organophosphate diisopropylfluorophosphate. Toxicol Sci. 2010; 116:623–31. [PubMed: 20498005]

Dolgin E. Syrian gas attack reinforces need for better anti-sarin drugs. Nat Med. 2013; 19:1194–5. [PubMed: 24100968]

Duffy BA, Chun KP, Ma D, Lythgoe MF, Scott RC. Dexamethasone exacerbates cerebral edema and brain injury following lithium-pilocarpine induced status epilepticus. Neurobiol Dis. 2014; 63:229–36. [PubMed: 24333865]

Fabene PF, Merigo F, Galie M, Benati D, Bernardi P, Farace P, et al. Pilocarpine-induced status epilepticus in rats involves ischemic and excitotoxic mechanisms. PLoS One. 2007; 2:e1105. [PubMed: 17971868]

Farr TD, Wegener S. Use of magnetic resonance imaging to predict outcome after stroke: a review of experimental and clinical evidence. J Cereb Blood Flow Metab. 2010; 30:703–17. [PubMed: 20087362]

Flannery BM, Bruun DA, Rowland DJ, Banks CN, Austin AT, Kukis DL, et al. Persistent neuroinflammation and cognitive impairment in a rat model of acute diisopropylfluorophosphate intoxication. J Neuroinflammation. 2016; 13:267. [PubMed: 27733171]

Gaidhani N, Sun F, Schreihofer D, Uteshev VV. Duration of isoflurane-based surgical anesthesia determines severity of brain injury and neurological deficits after a transient focal ischemia in young adult rats. Brain Res Bull. 2017; 134:168–76. [PubMed: 28755978]

Gale K. Progression and generalization of seizure discharge: anatomical and neurochemical substrates. Epilepsia. 1988; 29(Suppl 2):S15–34.

Gomes WA, Shinnar S. Prospects for imaging-related biomarkers of human epileptogenesis: a critical review. Biomark Med. 2011; 5:599–606. [PubMed: 22003908]

Grohn O, Pitkanen A. Magnetic resonance imaging in animal models of epilepsy-noninvasive detection of structural alterations. Epilepsia. 2007; 48(Suppl 4):3–10.

Gullapalli RP, Aracava Y, Zhuo J, Helal Neto E, Wang J, Makris G, et al. Magnetic resonance imaging reveals that galantamine prevents structural brain damage induced by an acute exposure of guinea pigs to soman. Neurotoxicology. 2010; 31:67–76. [PubMed: 19782102]

Gunnell D, Eddleston M. Suicide by intentional ingestion of pesticides: a continuing tragedy in developing countries. International Journal of Epidemiology. 2003; 32:902–9. [PubMed: 14681240]

Gunnell D, Eddleston M, Phillips MR, Konradsen F. The global distribution of fatal pesticide self-poisoning: systematic review. BMC Public Health. 2007; 7:357. [PubMed: 18154668]

Gupta, RC. Toxicology of Organophosphate & Carbamate Compounds. Burlington: Academic Press; 2006. CHAPTER 2 - Classification and Uses of Organophosphates and Carbamates; p. 5-24.

Heiss DR, Zehnder DW 2nd, Jett DA, Platoff GE Jr, Yeung DT, Brewer BN. Synthesis and Storage Stability of Diisopropylfluorophosphate. J Chem. 2016; 2016

Hertle D, Beynon C, Zweckberger K, Vienenkotter B, Jung CS, Kiening K, et al. Influence of isoflurane on neuronal death and outcome in a rat model of traumatic brain injury. Acta Neurochir Suppl. 2012; 114:383–6. [PubMed: 22327728]

Hobson BA, Siso S, Rowland DJ, Harvey DJ, Bruun DA, Garbow JR, et al. From the Cover: Magnetic Resonance Imaging Reveals Progressive Brain Injury in Rats Acutely Intoxicated With Diisopropylfluorophosphate. Toxicol Sci. 2017; 157:342–53. [PubMed: 28329842]

Jett DA. Neurological aspects of chemical terrorism. Ann Neurol. 2007; 61:9–13. [PubMed: 17262854]

Kaur S, Singh S, Chahal KS, Prakash A. Potential pharmacological strategies for the improved treatment of organophosphate-induced neurotoxicity. Can J Physiol Pharmacol. 2014; 92:893–911. [PubMed: 25348489]

Lanciego JL, Luquin N, Obeso JA. Functional neuroanatomy of the basal ganglia. Cold Spring Harb Perspect Med. 2012; 2:a009621. [PubMed: 23071379]

Li Y, Lein PJ, Liu C, Bruun DA, Tewolde T, Ford G, et al. Spatiotemporal pattern of neuronal injury induced by DFP in rats: a model for delayed neuronal cell death following acute OP intoxication. Toxicol Appl Pharmacol. 2011; 253:261–9. [PubMed: 21513723]

Liachenko S, Ramu J, Konak T, Paule MG, Hanig J. Quantitative Assessment of MRI T2 Response to Kainic Acid Neurotoxicity in Rats in vivo. Toxicol Sci. 2015; 146:183–91. [PubMed: 25904105]

Lin SP, Schmidt RE, McKinstry RC, Ackerman JJ, Neil JJ. Investigation of mechanisms underlying transient T2 normalization in longitudinal studies of ischemic stroke. J Magn Reson Imaging. 2002; 15:130–6. [PubMed: 11836767]

Liu C, Li Y, Lein PJ, Ford BD. Spatiotemporal patterns of GFAP upregulation in rat brain following acute intoxication with diisopropylfluorophosphate (DFP). Curr Neurobiol. 2012; 3:90–7. [PubMed: 24039349]

Lowenstein DH, Bleck T, Macdonald RL. It's time to revise the definition of status epilepticus. Epilepsia. 1999; 40:120–2. [PubMed: 9924914]

Makinen S, van Groen T, Clarke J, Thornell A, Corbett D, Hiltunen M, et al. Coaccumulation of calcium and beta-amyloid in the thalamus after transient middle cerebral artery occlusion in rats. J Cereb Blood Flow Metab. 2008; 28:263–8. [PubMed: 17653130]

Matchett GA, Allard MW, Martin RD, Zhang JH. Neuroprotective effect of volatile anesthetic agents: molecular mechanisms. Neurol Res. 2009; 31:128–34. [PubMed: 19298752]

McDonough JH Jr, Shih TM. Neuropharmacological mechanisms of nerve agent-induced seizure and neuropathology. Neurosci Biobehav Rev. 1997; 21:559–79. [PubMed: 9353792]

McDonough JH, McMonagle JD, Shih TM. Time-dependent reduction in the anticonvulsant effectiveness of diazepam against soman-induced seizures in guinea pigs. Drug Chem Toxicol. 2010; 33:279–83. [PubMed: 20429808]

Mendes A, Sampaio L. Brain magnetic resonance in status epilepticus: A focused review. Seizure. 2016; 38:63–7. [PubMed: 27156207]

Mew EJ, Padmanathan P, Konradsen F, Eddleston M, Chang SS, Phillips MR, et al. The global burden of fatal self-poisoning with pesticides 2006–15: Systematic review. J Affect Disord. 2017; 219:93–104. [PubMed: 28535450]

Milligan TA, Zamani A, Bromfield E. Frequency and patterns of MRI abnormalities due to status epilepticus. Seizure. 2009; 18:104–8. [PubMed: 18723376]

Mirsattari SM, Sharpe MD, Young GB. Treatment of refractory status epilepticus with inhalational anesthetic agents isoflurane and desflurane. Arch Neurol. 2004; 61:1254–9. [PubMed: 15313843]

Miyaki K, Nishiwaki Y, Maekawa K, Ogawa Y, Asukai N, Yoshimura K, et al. Effects of sarin on the nervous system of subway workers seven years after the Tokyo subway sarin attack. J Occup Health. 2005; 47:299–304. [PubMed: 16096354]

Morita H, Yanagisawa N, Nakajima T, Shimizu M, Hirabayashi H, Okudera H, et al. Sarin poisoning in Matsumoto, Japan. Lancet. 1995; 346:290–3. [PubMed: 7630252]

Myhrer T. Identification of neuronal target areas for nerve agents and specification of receptors for pharmacological treatment. Neurotoxicology. 2010; 31:629–38. [PubMed: 20624420]

Myhrer T, Aas P. Choice of approaches in developing novel medical countermeasures for nerve agent poisoning. Neurotoxicology. 2014; 44:27–38. [PubMed: 24820435]

Nairismagi J, Grohn OH, Kettunen MI, Nissinen J, Kauppinen RA, Pitkanen A. Progression of brain damage after status epilepticus and its association with epileptogenesis: a quantitative MRI study in a rat model of temporal lobe epilepsy. Epilepsia. 2004; 45:1024–34. [PubMed: 15329065]

Nakasu Y, Nakasu S, Morikawa S, Uemura S, Inubushi T, Handa J. Diffusion-weighted MR in experimental sustained seizures elicited with kainic acid. AJNR Am J Neuroradiol. 1995; 16:1185–92. [PubMed: 7677009]

Odaka H, Numakawa T, Adachi N, Ooshima Y, Nakajima S, Katanuma Y, et al. Cabergoline, dopamine D2 receptor agonist, prevents neuronal cell death under oxidative stress via reducing excitotoxicity. PLoS One. 2014; 9:e99271. [PubMed: 24914776]

Paxinos, G. The rat brain in stereotaxic coordinates. 6. Amsterdam ; Boston: Amsterdam ; Boston: Elsevier; 2007.

Pereira EF, Aracava Y, DeTolla LJ Jr, Beecham EJ, Basinger GW Jr, Wakayama EJ, et al. Animal models that best reproduce the clinical manifestations of human intoxication with organophosphorus compounds. J Pharmacol Exp Ther. 2014; 350:313–21. [PubMed: 24907067]

Pessah IN, Rogawski MA, Tancredi DJ, Wulff H, Zolkowska D, Bruun DA, et al. Models to identify treatments for the acute and persistent effects of seizure-inducing chemical threat agents. Ann N Y Acad Sci. 2016; 1378:124–36. [PubMed: 27467073]

Pouliot W, Bealer SL, Roach B, Dudek FE. A rodent model of human organophosphate exposure producing status epilepticus and neuropathology. Neurotoxicology. 2016; 56:196–203. [PubMed: 27527991]

Puyal J, Ginet V, Clarke PG. Multiple interacting cell death mechanisms in the mediation of excitotoxicity and ischemic brain damage: a challenge for neuroprotection. Prog Neurobiol. 2013; 105:24–48. [PubMed: 23567504]

Roch C, Leroy C, Nehlig A, Namer IJ. Magnetic resonance imaging in the study of the lithium-pilocarpine model of temporal lobe epilepsy in adult rats. Epilepsia. 2002; 43:325–35. [PubMed: 11952761]

Rodriguez MJ, Pugliese M, Mahy N. Drug abuse, brain calcification and glutamate-induced neurodegeneration. Curr Drug Abuse Rev. 2009; 2:99–112. [PubMed: 19630740]

Rojas A, Ganesh T, Manji Z, O'Neill T, Dingledine R. Inhibition of the prostaglandin E2 receptor EP2 prevents status epilepticus-induced deficits in the novel object recognition task in rats. Neuropharmacology. 2016; 110:419–30. [PubMed: 27477533]

Rosman Y, Eisenkraft A, Krivoy A, Schein O, Makarovski I, Shrot S, et al. Using MRI for the assessment of paraoxon-induced brain damage and efficacy of antidotal treatment. J Appl Toxicol. 2012; 32:409–16. [PubMed: 21861267]

Shrot S, Anaby D, Krivoy A, Makarovsky I, Rosman Y, Bloch-Shilderman E, et al. Early in vivo MR spectroscopy findings in organophosphate-induced brain damage-potential biomarkers for short-term survival. Magn Reson Med. 2012; 68:1390–8. [PubMed: 22247007]

Shrot S, Tauber M, Shiyovich A, Milk N, Rosman Y, Eisenkraft A, et al. Early brain magnetic resonance imaging can predict short and long-term outcomes after organophosphate poisoning in a rat model. Neurotoxicology. 2015; 48:206–16. [PubMed: 25912464]

Siso S, Hobson BA, Harvey DJ, Bruun DA, Rowland DJ, Garbow JR, et al. Editor's Highlight: Spatiotemporal Progression and Remission of Lesions in the Rat Brain Following Acute Intoxication With Diisopropylfluorophosphate. Toxicol Sci. 2017; 157:330–41. [PubMed: 28329845]

Stokum JA, Gerzanich V, Simard JM. Molecular pathophysiology of cerebral edema. J Cereb Blood Flow Metab. 2016; 36:513–38. [PubMed: 26661240]

Suleymanova EM, Gulyaev MV, Abbasova KR. Structural alterations in the rat brain and behavioral impairment after status epilepticus: An MRI study. Neuroscience. 2016; 315:79–90. [PubMed: 26674057]

Testylier G, Lahrech H, Montigon O, Foquin A, Delacour C, Bernabe D, et al. Cerebral edema induced in mice by a convulsive dose of soman. Evaluation through diffusion-weighted magnetic resonance imaging and histology. Toxicol Appl Pharmacol. 2007; 220:125–37. [PubMed: 17350063]

Vaarmann A, Kovac S, Holmstrom KM, Gandhi S, Abramov AY. Dopamine protects neurons against glutamate-induced excitotoxicity. Cell Death Dis. 2013; 4:e455. [PubMed: 23303129]

Vismer MS, Forcelli PA, Skopin MD, Gale K, Koubeissi MZ. The piriform, perirhinal, and entorhinal cortex in seizure generation. Front Neural Circuits. 2015; 9:27. [PubMed: 26074779]

Zeiler FA, Zeiler KJ, Teitelbaum J, Gillman LM, West M. Modern inhalational anesthetics for refractory status epilepticus. Can J Neurol Sci. 2015; 42:106–15. [PubMed: 25572922]

## Highlights

- Acute DFP intoxication rapidly elicits *status epilepticus* (SE) in adult male rats
- T2w MRI revealed lesions in multiple brain regions beginning 6 h post-exposure
- Onset and progression of DFP-induced lesions varied across brain regions
- Isoflurane anesthesia attenuated lesion severity in a region-dependent manner
- Longitudinal MRI may be a powerful tool for assessing therapeutic response

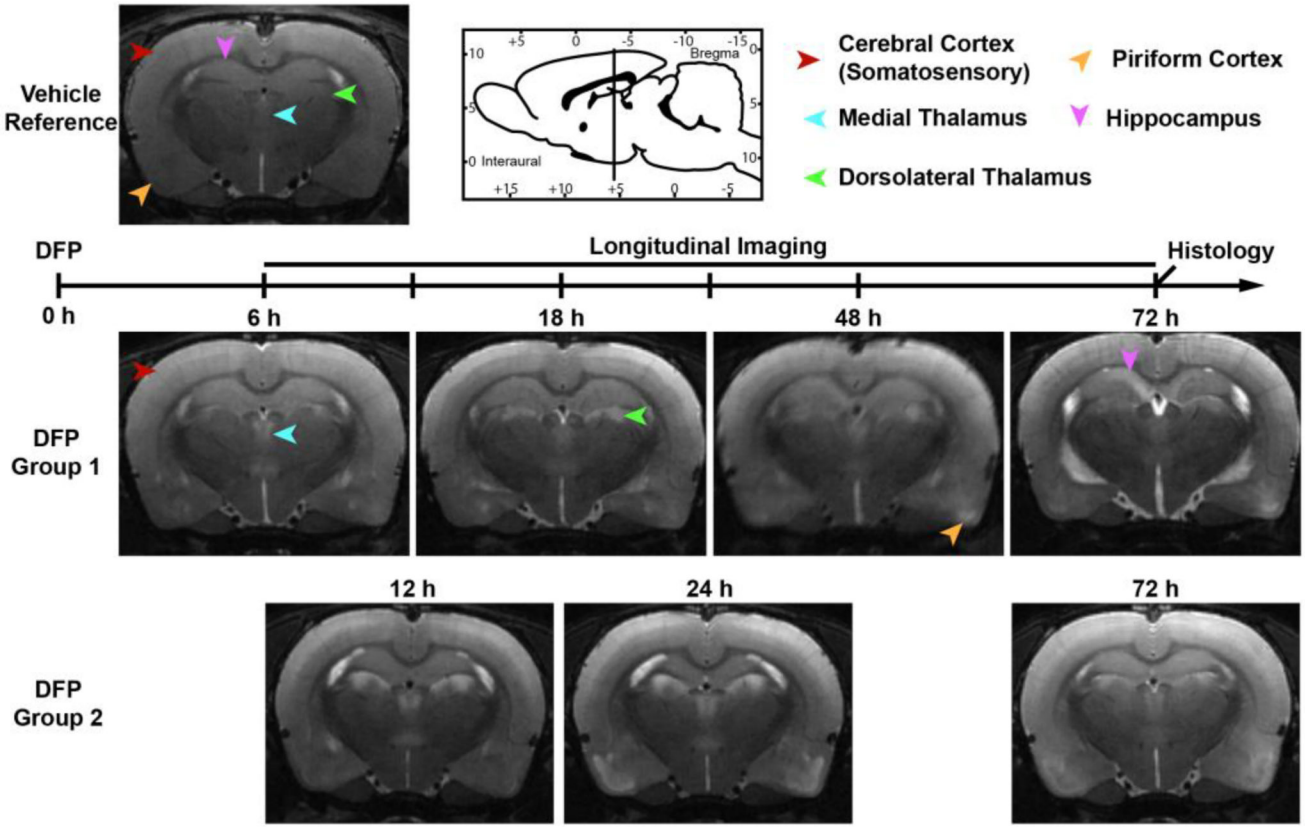


**Figure 1. T2w anatomic MR images depicting the spatiotemporal progression of brain lesions following acute DFP intoxication**

Lesions were characterized by localized hyperintensity compared to neighboring tissue, and a vehicle control reference scan. Group 1 and Group 2 images each represent a single animal imaged at 6, 18, 48 and 72 h, or 12, 24 and 72 h respectively. Note that Group 1 begins MR imaging 6 h prior to Group 2. Across time points, images were selected to match bregma to ≤ 250 μm. Arrows indicate the positions of brain regions displaying hyperintense lesions at one or more time points following intoxication. Sagittal-view atlas reference was adapted from Watson and Paxinos, *The Rat Atlas in Stereotactic Coordinates* (Paxinos, 2007).

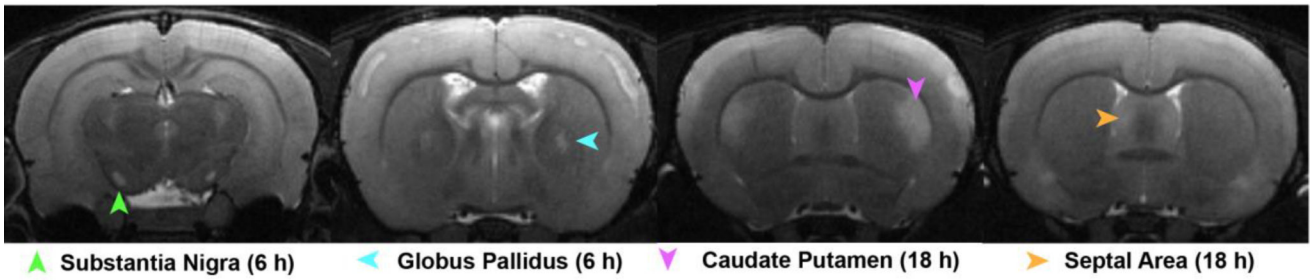


**Figure 2. T2w anatomic MR images depicting brain regions with sporadic lesions across study animals**

Images of lesions in the septal area, caudate putamen, globus pallidus, and substantia nigra collected from Group 1 animals. The images displaying the substantia nigra and caudate putamen lesions are from the same animal at two separate time points; the other images are each from separate animals.

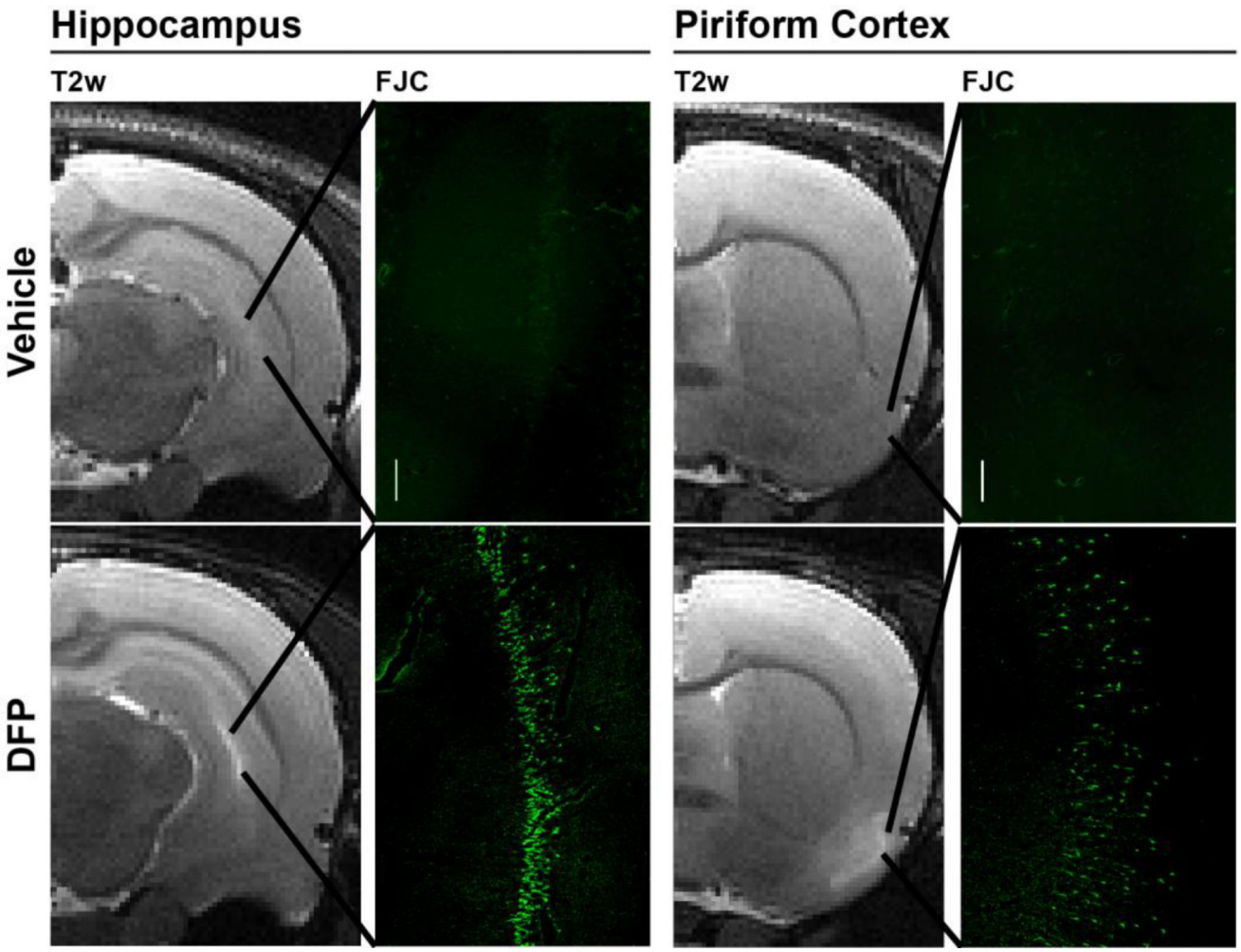


**Figure 3. Lesions detected by T2w MRI at 72 h post DFP intoxication correspond to regions of ongoing neurodegeneration as assessed by FluoroJade C (FJC) staining**

The vehicle control animal shows *no* T2w hyperintensity or FJC positive neurons in the hippocampus or piriform cortex. In contrast, DFP intoxication produced hyperintensity in the hippocampus and piriform cortex that shows spatial registry to bands of FJC positive cells. Magnification: 100×.

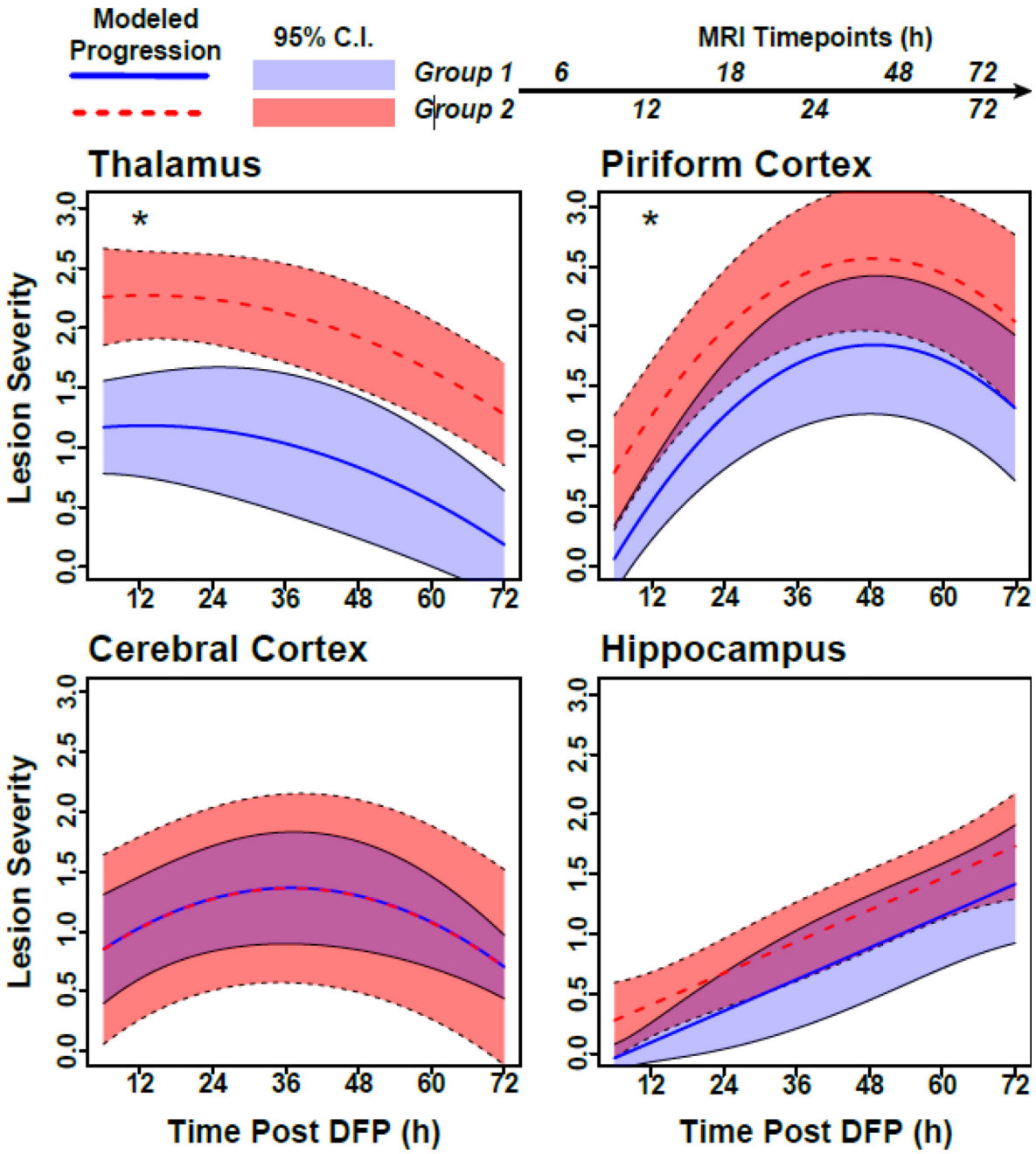


**Figure 4. Mixed-model regression from multiple brain regions demonstrate that the lesion severity changes over time in a brain-region and imaging group-dependent manner**

Each progression curve is modeled on data from six animals from Group 1 (solid lines) or six animals from Group 2 (dashed lines). 95% confidence bands are included around the curves for each imaging group. Group 1 animals had significantly lower lesion severity scores for the thalamus and piriform cortex than Group 2 animals over the entire study period (denoted with an "*"). Note: Group 1 animals received anesthesia 6 h earlier than Group 2 animals.

**Table 1**

Summary of MRI lesion severity scores.

| Time Post DFP (h) | 6* | | 12** | | 18* | | 24** | | 48* | | 72*** | |
|---|---|---|---|---|---|---|---|---|---|---|---|---|
| | Incidence | Severity | Incidence | Severity | Incidence | Severity | Incidence | Severity | Incidence | Severity | Incidence | Severity |
| Hippocampus | 0/6 | n/a | 4/6 | 0.6 ± 0.4 | 4/6 | 0.2 ± 0.0 | 5/6 | 0.7 ± 0.5 | 5/5 | 0.9 ± 0.7 | 11/11 | 1.5 ± 0.8 |
| Piriform Cortex | 4/6 | 0.2 ± 0.0 | 6/6 | 1.2 ± 0.5 | 3/6 | 1.1 ± 1.0 | 6/6 | 2.3 ± 0.8 | 5/5 | 1.8 ± 0.6 | 10/11 | 1.9 ± 0.9 |
| Thalamus | 6/6 | 1.0 ± 0.5 | 6/6 | 2.6 ± 0.3 | 5/6 | 1.1 ± 0.7 | 6/6 | 2.2 ± 0.6 | 5/5 | 0.9 ± 0.8 | 10/11 | 0.8 ± 0.5 |
| Cerebral Cortex | 6/6 | 0.5 ± 0.6 | 6/6 | 1.2 ± 1.0 | 6/6 | 1.7 ± 0.9 | 5/6 | 1.4 ± 1.0 | 5/5 | 0.9 ± 0.6 | 7/11 | 1.2 ± 0.7 |
| Substantia Nigra | 3/6 | 1.4 ± 0.8 | 1/6 | 0.2 (n=1) | 3/6 | 1.5 ± 0.9 | 1/6 | 0.2 (n=1) | 1/5 | 1.2 (n=1) | 2/11 | 0.7 ± 0.7 |
| Caudate Putamen | 0/6 | n/a | 1/6 | 0.2 (n=1) | 5/6 | 1.0 ± 0.8 | 2/6 | 0.2 ± 0.0 | 3/5 | 0.7 ± 0.4 | 2/11 | 0.6 ± 0.5 |
| Lateral Ventricles | 0/6 | n/a | 6/6 | 0.5 ± 0.2 | 2/6 | 0.6 ± 0.5 | 5/6 | 1.1 ± 0.4 | 0/5 | n/a | 5/11 | 1.3 ± 0.8 |

Incidence represents the fraction of animals with observable lesions at any given time post-DFP injection; severity, the average lesion severity score of animals with lesions at any given time point presented as the mean ± SD (animals without lesions were not included in the calculation of the average lesion severity score). N/A, no animals presented with lesions at any given time point; (n=1), data represents score from a single animal;

*Includes only animals in Group 1;

**, only animals in Group 2;

***Combined data from Group 1 and Group 2.